^{113}Cd Shielding Tensors of Cadmium Compounds. 7. X-ray Structure and ^{113}Cd NMR Studies of Poly(bis(acetato)bis(imidazole)cadmium(II)). A Model Compound for Cd-Substituted Carboxypeptidase-A and Thermolysin

Edwin Rivera, Michael A. Kennedy, Richard D. Adams,* and Paul D. Ellis*

Contribution from the Department of Chemistry, University of South Carolina, Columbia, South Carolina 29208. *Received June 30, 1989*

Abstract: The structure of poly(bis(acetato)bis(imidazole)cadmium(II)) [$Cd(OAc)_2(Im)_2$] was determined by X-ray diffraction methods. $Cd(OAc)_2(Im)_2$ crystallizes in the space group $P2_1/c$, and the monoclinic unit cell constants are a = 7.6563 Å, b = 10.2048 Å, c = 17.5709 Å, β = 95.764°, Z = 4. The coordination about the metal atom is best described as a distorted octahedron. The two imidazole ligands and an asymmetrical chelating acetate ligand define an equatorial plane. The axial positions are occupied by two monodentate acetate ligands that form bridges to the neighboring metal atoms producing infinite chains. ^{113}Cd solid-state NMR experiments were performed on $Cd(OAc)_2(Im)_2$ to determine the magnitude and orientation of the ^{113}Cd shielding tensor. The principle elements of the shielding tensor determined from both powder and oriented single-crystal experiments in the molecular frame of $Cd(OAc)_2(Im)_2$ are σ_{11} = -40.62 ppm, σ_{22} = 101.37 ppm, and σ_{33} = 248.75 ppm. As anticipated from the crystal symmetry, two symmetry-related tensors were observed in the single-crystal experiment. Some simple empirical rules provided a vehicle for the assignment of the symmetry-related tensors to lattice sites. The most deshielded element σ_{33} is 75° off the plane containing the two imidazole nitrogens and cadmium metal ion, while the most shielded element σ_{11} is 63° from the best least-squares line containing the axial Cd-O bonds. The results presented in this paper can be utilized in predicting the orientation of the ^{113}Cd shielding tensor in Cd-substituted carboxypeptidase-A. Since the enzyme thermolysin has a similar metal environment as carboxypeptidase-A, $Cd(OAc)_2(Im)_2$ may also be used as a model compound of Cd-substituted thermolysin. This work represents part of our ongoing investigation on ^{113}Cd shielding tensors via single-crystal NMR experiments on model compounds resembling the metal environment of metalloproteins.

In 1976[1] Armitage introduced ^{113}Cd as an NMR spin spy in metalloproteins. The ^{113}Cd nucleus is a good metallobioprobe because it has favorable NMR properties[2,3] and similar physical properties as some of the native metals, e.g., Zn^{2+}, Ca^{2+}, and Mg^{2+}. For example, the relative receptivity for ^{113}Cd (I = 1/2) is 155 compared to ^{43}Ca (I = 7/2), 5 compared to ^{25}Mg (I = 5/2), and 11 compared to ^{67}Zn (I = 5/2). The metal ion plays an important role in the catalytic mechanism of some enzymes. Upon substitution of the native metal ion with ^{113}Cd, the activity is partially or fully restored. The original studies[1-4] on Cd-substituted proteins were performed in the liquid state. In liquids, only the average of the shielding tensor is observable due to the rapid tumbling of the molecules. The isotropic chemical shift determined in liquids is influenced by exchange processes, temperature, concentration, and solvent effects which may limit the interpretation of the structural changes taking place at the metal site during inhibition.

By performing the experiments in the solid state complete information concerning the shielding tensor can be obtained in principle without the potential difficulties mentioned above. The principal elements of the shielding tensor can be extracted from NMR experiments on powder samples.[5] The complete shielding tensor including its orientation with respect to a molecule fixed coordinate system is obtained from single-crystal NMR experiments.[6] The use of model compounds for proteins is necessary for several reasons, e.g., protein single crystals are generally too small and at times are unstable in the absence of the mother liquor. The most significant restriction to performing single-crystal experiments on protein single crystals is the low percentage by weight of ^{113}Cd relative to that of the protein. This situation for single crystals leads to prohibitively long data collection times. Hence, we have employed powder samples to obtain the elements of the shielding tensor. These studies are combined with single studies on appropriate model compounds to obtain information concerning the orientation of the shielding tensor at the metal site in metalloproteins.[6]

Honkonen, Doty, and Ellis[7] first reported studies of ^{113}Cd shielding tensors for model compounds which resemble the metal environment of proteins containing an all-oxygen coordination. Such Cd-oxo environments are found in the proteins parvalbumin, skeletal troponin-C, and concanavalin. From these studies a series of structural/chemical shift correlations were deduced:[7c] (1) tensor elements with similar values have similar orthogonal environments; (2) the most shielded element is aligned nearly perpendicular to the longest Cd-O bond; (3) the most deshielded element is aligned most perpendicular to a plane containing water oxygen or in the absence of water molecules is oriented in such a way to maximize the deshielding contribution of the shortest cadmium-oxygen bond. In addition, an additivity model for determining the shielding contribution to the Cd nucleus by various ligand types was developed.[7b] Our interest in studying metalloproteins having mixed nitrogen/oxygen Cd coordination has necessitated an extension of our studies on ^{113}Cd shielding tensors via single-crystal NMR to include model compounds resembling the metal site of these metalloproteins.

The ^{113}Cd shielding tensors of cadmium complexes with ligands containing mixed nitrogen/oxygen donor atoms[7c-9] have been studied as model compounds for proteins containing similar mixed

(1) Armitage, I. M.; Pajer, R. T.; Uiterkamp, A. J. M. S.; Chelebowski, J. F.; Coleman, J. E. *J. Am. Chem. Soc.* **1976**, *98*, 5710.
(2) Summers, M. F. *Coord. Chem. Revs.* **1988**, *86*, 43.
(3) Ellis, P. D. *Science* **1983**, *221*, 1141.
(4) (a) Armitage, I. M.; Uiterkamp, A. J. M. S.; Chelebowski, J. F.; Coleman, J. E. *J. Magn. Reson.* **1978**, *29*, 375. (b) Chlebowski, J. F.; Coleman, J. E. *Adv. Inorg. Biochem.* **1979**, *1*, 1-66. (c) Gettins, P.; Coleman, J. E. *Fed. Proc.* **1982**, *41(13)*, 2966.
(5) Marchetti, P. S.; Ellis, P. D.; Bryant, R. G. *J. Am. Chem. Soc.* **1985**, *107*, 8191.
(6) Kennedy, M. A.; Ellis, P. D. *Concepts Magn. Reson.* **1989**, *1*, 35-47. In press.
(7) (a) Honkonen, R. S.; Doty, F. D.; Ellis, P. D. *J. Am. Chem. Soc.* **1983**, *105*, 4163. (b) Honkonen, R. S.; Marchetti, P. S.; Ellis, P. D. *J. Am. Chem. Soc.* **1984**, *106*, 5488. (c) Honkonen, R. S.; Ellis, P. D. *J. Am. Chem. Soc.* **1986**, *108*, 912. (d) Marchetti, P. S.; Honkonen, R. S.; Ellis, P. D. *J. Magn. Reson.* **1987**, *71*, 294.
(8) (a) Kennedy, M. A.; Ellis, P. D. *J. Inorg. Chem.* Submitted for publication. (b) Kennedy, M. A.; Ellis, P. D. Submitted to *J. Inorg. Chem.*
(9) Munakata, M.; Kitagawa, S.; Yagi, F. *Inorg. Chem.* **1986**, *25*, 964.

0002-7863/90/1512-1400$02.50/0 © 1990 American Chemical Society

nitrogen/oxygen coordination. In 1980, Horrocks[10] first introduced a set of Co(II) and Zn(II) model compounds to compare the visible and the magnetic circular dichroism spectra of the Co-substituted, native Zn carboxypeptidase-A [CPA] and thermolysin [TL]. In this paper we introduce a similar Cd(II) model compound, poly(bis(acetato)bis(imidazole)cadmium(II)) [Cd$(OAc)_2(Im)_2$], which contains a mixed nitrogen/oxygen coordination resembling the metal environment of Cd-substituted CPA and TL. The impetus for the ^{113}Cd shielding tensor studies of ^{113}Cd-substituted CPA[11] and TL[12] is to understand the nature of the ^{113}Cd isotropic chemical shift observed in the presence and absence of inhibitors in the liquid state.[13] An understanding of the changes that are taking place at the metal site when a substrate binds during the catalytic action of these enzymes can be interpreted in terms of the structural factors which determine the magnitude and orientation of the ^{113}Cd shielding tensors of CPA and TL. The structural changes at the metal site will be reflected by the changes in the magnitude of the individual elements of the shielding tensor. The isotropic chemical shift may not reflect the changes at the metal site due to the possibility that the individual tensor elements may move in opposite directions.[14] To be able to correlate shielding tensor information to biologically important enzymatic mechanisms is one of the aims of our ongoing investigation of ^{113}Cd shielding tensors by single-crystal NMR experiments.

Experimental Section

Materials. $Cd(OAc)_2(H_2O)_2$ was purchased from Aldrich Chem. Co. and was used without further purification. Imidazole was purchased from Sigma Chemical Co. and was recrystallized twice in H_2O before use. Ethanol was purchased from USI Chem. Co.

Crystal Preparation. The cadmium complex described in this paper was synthesized by using similar procedures as those described for the synthesis of the analogous Zn and Co complexes.[10] [$Cd(OAc)_2(Im)_2$] was prepared by dissolving 2 mL of glacial acetic acid (12 M) and 18.19 g (68.1 mmol) of [$Cd(OAc)_2(H_2O)_2$] in 200 mL of 95% ethanol at reflux. Imidazole, 9.27 g (136.16 mmol), was dissolved in 100 mL of 95% ethanol and added dropwise to the reflux solution. After 2 h of refluxing, the solution was separated into approximately 50-mL alliquots. Crystals obtained by evaporating at room temperature were small, brittle, and unsuitable for single-crystal NMR experiment. After various reseeding processes crystals of a suitable size (4 × 4 × 3 mm) were obtained at 4 °C and used in the NMR single-crystal experiment. Crystals grown at 4 °C were also used for X-ray structural determination.

Crystallographic Analysis. The data crystal for X-ray analysis was cleaved from a very large crystal and was mounted on a thin glass capillary. Diffraction measurements were made on a Rigaku AFC6 automatic diffractometer by using graphite-monochromatized Mo Kα radiation. The unit cell constants were determined from 25 randomly selected reflections obtained by using an AFC6 automatic search, center index, and least-squares routines. All data processing was performed on a Digital Equipment Corp. MICROVAX II computer by using the Texsan structure solving program library (version 2.0) obtained from Molecular Structure Corp., The Woodlands, TX. Neutral atoms scattering factors were calculated by the standard procedure.[15a] Anomalous dispersion corrections were applied to all non-hydrogen atoms.[15b] Full-matrix least-squares refinements minimized the function:

$$\sum_{hkl} w(|F_{obs}| - |F^2_{calc}|) \tag{1}$$

where

$$w = 1/\sigma(F)^2$$

$$\sigma(F) = \sigma(F^2_{obs})/2F_{obs}$$

$$\sigma(F^2_{obs}) = [\sigma(I_{raw})^2 + (0.02F^2_{obs})^2]^{1/2}/\mathrm{Lp}$$

(10) Horrocks, W. DeW., Jr.; Ishley, J. N.; Barton, H.; Thompson, J. S. *J. Inorg. Biochem.* **1980**, *12*, 131–141.
(11) Gettins, P. *J. Biol. Chem.* **1986**, *261*(33), 15513.
(12) Gettins, P. *J. Biol. Chem.* **1988**, *263*(21), 10208.
(13) Ellis, P. D. *J. Biol. Chem.* **1989**, *264*(6), 3108.
(14) Kennedy, M. A.; Ellis, P. D. *J. Am. Chem. Soc.* **1989**, *111*, 3195.
(15) *International Tables for X-ray Crystallography* (*I.T.C.*); Kynoch Press: Birmingham, England, 1975; Vol. IV. (a) Table 2.2B, pp 99–101. (b) Table 2.31, pp 149–150.

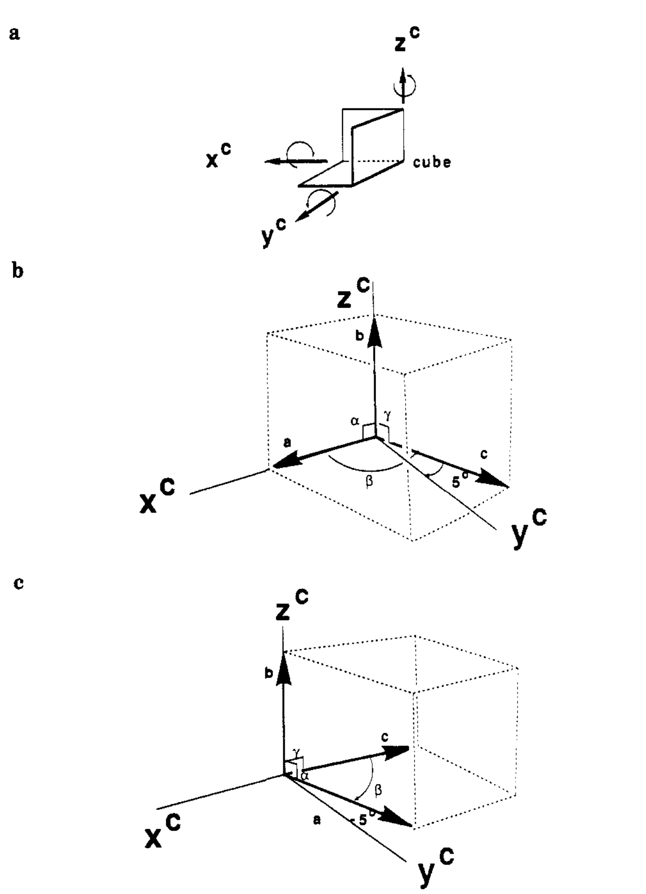

Figure 1. a. An illustration of the opened three-sided cube. The single crystal is mounted on a ceramic cube, and rotations are performed perpendicular to the field B_0 about each of the axes x^c, y^c, and z^c. b. Illustrates the orientation of the natural unit cell axes of $Cd(OAc)_2(Im)_2$ crystal selected in this experiment with respect to the orthogonal cube axes. The unit cell is depicted in a left-handed coordinate system. c. The conversion to a right-handed coordinate system with respect to the cubeframe was performed by adding 90° to the non-Euler γ angle.

where F is the structure factor, w is a weight of each term, Lp is the Lorentz polarization factor, σ is the standard deviation, and h,k,l are the Miller indices.

$Cd(OAc)_2(Im)_2$ crystallized in the monoclinic crystal system. The space group $P2_1/c$ was determined from systematic absences observed during the data collection. An empirical absorption correction was applied to the data. The structure was solved by a combination of direct methods (MITHRIL) and difference Fourier syntheses. All non-hydrogen atoms were refined by using anisotropic thermal parameters. Hydrogen atom positions were calculated by assuming idealized geometries and employing observed positions whenever possible. The contribution of these hydrogen atoms were added to the structure factor calculations, but their positions were not refined. Error analysis were calculated from the inverse matrix obtained on the final cycle of refinement. See Supplementary Material for the tables of the structure factor amplitudes, tables of atomic positional parameters and the values of the anisotropic thermal parameters.

^1H and ^{13}C NMR. ^1H liquid and ^{13}C high-resolution solid-state NMR were used in addition to X-ray diffraction to characterize $Cd(OAc)_2(Im)_2$. The liquid-phase ^1H and solid-state ^{13}C NMR spectra of $Cd(OAc)_2(Im)_2$ were collected at 60 MHz on an Varian EM-360 spectrometer and at 75.72 MHz on an Varian XL-300 spectrometer, respectively. The ^1H chemical shifts for $Cd(OAc)_2(Im)_2$ relative to TMS at room temperature were (H_3C–, δ = 1.8 ppm), (–HC=CH–, δ = 7.0 ppm), and (–HC=N–, δ = 7.6 ppm). The isotropic ^{13}C chemical shifts relative to TMS at room temperature were (H_3C–, δ = 22 ppm), (N=C–N, δ = 140 ppm), (–C–N–, δ = 123.5 ppm), (–C–N=, δ = 118 ppm), and (–COO$^-$, δ = 180 ppm).

^{113}Cd NMR. All solid-state ^{113}Cd NMR experiments were performed on a Varian XL-300 in a narrow bore Varian Magnet at 7.05 T with a Larmor frequency for ^{113}Cd nucleus of 66.547 MHz. All chemical shifts are reported relative to $Cd(ClO_4)_2$. For MAS experiments, the sample was ground in a mortar and packed in a 7 mm o.d. macor rotor and spun at speeds of 3–5 KHz in a MAS probe purchased from Doty Scientific (Columbia, SC). The single-crystal experiment was performed by first

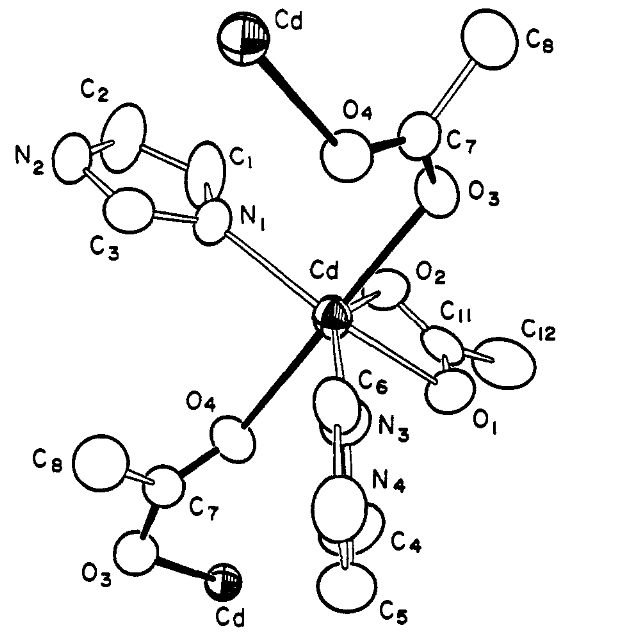

Figure 2. An ORTEP diagram of $Cd(OAc)_2(Im)_2$ showing the coordination about cadmium and bridging acetates ligands to the neighboring cadmium atoms in the polymeric chain.

mounting the $Cd(OAc)_2(Im)_2$ crystal on an open three-sided ceramic cube. The axes of the cube were labeled as x^c, y^c, and z^c as shown in Figure 1a. To minimize the contact with air and moisture the crystal was protected with an acrylic coating. Alignment of the natural b and c axes of the monoclinic unit cell (following the convention of Rollett[16]) with respect to the orthogonal cube frame was accomplished by a combination of Weissenberg oscillations and Laue camera techniques.[17] The source of X-rays for the crystal alignment was Cu Kα radiation (λ_α = 1.542 Å).

Upon crystal alignment, the unit cell axes a^* and b were found to be collinear with the x^c and z^c axes of the cube, respectively, while the c^* axis was found to be 5° off the y^c axis of the cube see Figure 1b. To maintain the right-handed coordinate system convention it was necessary to add 90° to $\gamma = -5° + 90° = 85°$, see Figure 1c. The cube z^c axis is collinear with the crystal 2-fold axis.[18] The rotation about x^c and z^c axes can also be viewed as rotations that are normal to the crystal planes (100) and the (010), respectively. The transformation matrix that orthogonalizes the natural monoclinic cell axes (a, b, c) into (a^*, b, c^*) is determined by eq 2 (Rollett[16])

$$\begin{pmatrix} u_1^* \\ u_2 \\ u_3^* \end{pmatrix} = \begin{pmatrix} a \sin \beta & 0 & 0 \\ 0 & b & 0 \\ a \cos \beta & 0 & c \end{pmatrix} \begin{pmatrix} u_1 \\ u_2 \\ u_3 \end{pmatrix} \quad (2)$$

where a, b, and c are the dimensions of the unit cells, u_1, u_2, and u_3 are coordinates in the natural unit cell basis, and u_1^*, u_2, and u_3^* are the corresponding coordinates in the orthogonalized basis.

Once aligned, the crystal was placed on a cube holder and mounted on the goniometer of a Doty Scientific single crystal probe. The starting position (0°) of each rotation plot is based on Mehring's[19] convention. The chemical shift-angle dependence was obtained by performing the rotations of the crystal in intervals of about 9° about each cube axis oriented perpendicular to the magnetic field B_0.

The data acquisition was via a standard single contact Hartmann-Hahn cross-polarization pulse sequence.[20] The proton 90° pulse was 4.5 and 8.0 μs for the single-crystal and MAS experiments, respectively. The optimized contact time was 6000 μs, and the recycle delay was 2 s. Finally, simulation of the MAS spectra was performed by using a program introduced by Marchetti et al.[21] based on the theory of Maricq and Waugh.[22] The best estimate for the shielding tensor parameters was obtained via a Simplex optimization[21] routine of the experimental side band intensities.

Table I. Positional Parameters and B(eq) for Bis(imidazoyl)cadmium Acetate

atom	x	y	z	B(eq)
Cd	0.08051 (5)	0.20045 (4)	0.22192 (2)	2.41 (2)
O1	0.3176 (5)	0.0632 (4)	0.2168 (2)	3.6 (2)
O2	0.1655 (5)	0.0771 (4)	0.1051 (2)	3.8 (2)
O3	0.2334 (5)	0.3703 (4)	0.1745 (2)	3.1 (2)
O4	−0.0793 (5)	0.0043 (4)	0.2599 (2)	3.1 (2)
N1	−0.1722 (6)	0.2544 (5)	0.1531 (3)	2.8 (2)
N2	−0.4459 (5)	0.3128 (5)	0.1258 (3)	3.2 (2)
N3	0.1376 (6)	0.2279 (5)	0.3482 (2)	2.8 (2)
N4	0.1543 (6)	0.3041 (6)	0.4652 (2)	3.5 (2)
C1	−0.2197 (8)	0.2342 (8)	0.0775 (3)	4.9 (4)
C2	−0.3886 (8)	0.2689 (8)	0.0601 (3)	5.1 (4)
C3	−0.3121 (8)	0.3025 (7)	0.1796 (3)	3.7 (3)
C4	0.1729 (8)	0.1259 (7)	0.3989 (4)	4.0 (3)
C5	0.1826 (8)	0.1705 (7)	0.4701 (3)	3.9 (3)
C6	0.1254 (7)	0.3349 (6)	0.3908 (3)	2.9 (3)
C7	0.1898 (7)	0.4839 (6)	0.1942 (3)	2.6 (3)
C8	0.2811 (8)	0.5948 (7)	0.1595 (4)	4.2 (3)
C11	0.2953 (8)	0.0366 (6)	0.1469 (4)	3.1 (3)
C12	0.431 (1)	−0.0467 (7)	0.1146 (4)	5.7 (4)

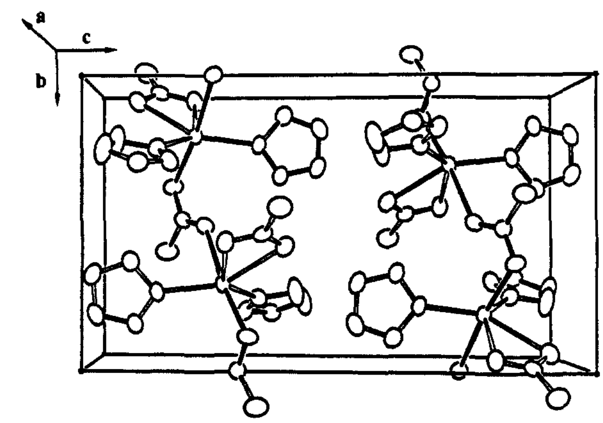

Figure 3. A perspective view of the unit cell of $Cd(OAc)_2(Im)_2$. The polymeric chains are indicated by solid bonds.

Results and Discussion

Description of the Solid-State Structure of $Cd(OAc)_2(Im)_2$. Unlike its Zn homolog which consists of discrete molecular units $Zn(OAc)_2Im_2$ with monodentate acetate ligands and a tetrahedral coordination about the Zn atom,[23] $Cd(OAc)_2(Im)_2$ consists of hexacoordinate cadmium groupings linked into infinite chains by bridging acetate ligands. An ORTEP diagram of one formula unit of the cadmium complex together with one bridging acetate is shown in Figure 2. The backbone of the polymer is shown by the series of solid bonds. Fractional atomic coordinates are listed in Table I. The coordination about the cadmium ion is best described as a distorted octahedron. An equatorial plane can be described by the asymmetrical chelating acetate and two nitrogen-coordinated imidazole ligands. The bridging acetate ligand occupies an axial position with respect to this plane. The Cd–O distances are significantly different, i.e., Cd–O(1) = 2.302 (4) and Cd–O(2) = 2.547 (4) Å. Asymmetrical chelating acetate ligands[24] with similar Cd–O distances were also observed in $Cd(OAc)_2(H_2O)_2$.[25] The Cd–N bond distances to the imidazole

(16) Rollett, J. S. *Computer Methods in Crystallography*; Pergamon Press: New York, 1975; p 22.
(17) Ladd, M. F. C.; Palmer, R. A. *Structure Determination by X-ray Crystallography*; 2nd ed.; Plemium Press: New York and London.
(18) The improper crystallographic 2-fold axis and the glide plane present in the space group $P2_1/c$ are referred to in this paper as the crystal 2-fold axis. Such a designation follows since the NMR experiment is independent of translation within the unit cell.
(19) Mehring, M. *High Resolution NMR in Solids*, 2nd ed., Springer-Verlag: Berlin, 1983.
(20) Pines, A.; Gibby, M. E.; Waugh, J. S. *Chem. Phys.* **1973**, *59*, 569.
(21) Marchetti, P. S.; Ellis, P. D.; Bryant, R. G. *J. Am. Chem. Soc.* **1985**, *107*, 8191.
(22) Maricq, M. M.; Waugh, J. S. *J. Chem. Phys.* **1979**, *70*(7), 3300.
(23) Horrocks, W. D., Jr.; Ishely, J. N.; Whittle, R. R. *Inorg. Chem.* **1982**, *21*, 3265.
(24) Brown, I. D. *J. Chem. Soc., Dalton Trans.* **1980**, 1118.

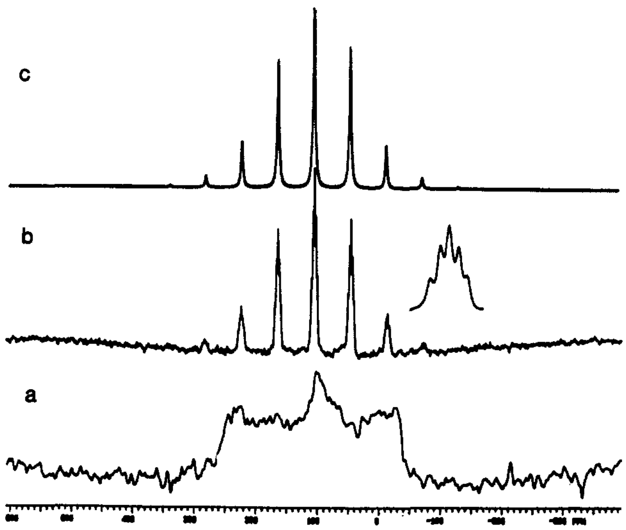

Figure 4. 66.547 MHz ^{113}Cd spectra of $Cd(OAc)_2(Im)_2$. a. Static. b. Spun at 4.0 KHz. Inset shows the splitting produced by the dipolar coupling between ^{14}N and ^{113}Cd. c. Simulated MAS spectra of $Cd(OAc)_2(Im)_2$, part b. Dipolar couplings to the ^{113}Cd nucleus have been ignored.

Table II. ^{113}Cd Shielding Tensor Parameters from MAS Spectra of $Cd(OAc)_2(Im)_2$

tensor elements (ppm)	isotropic chemical shift δ (ppm)	anisotropy $\Delta\sigma$ (ppm)	assymmetry parameter η
σ_{11} = −40.0 σ_{22} = 101.4 σ_{33} = 248.8	103.4	221.38	0.921

ligands, 2.235 (4) and 2.245 (4) Å, are not unusual.[26] The bridging acetate ligand possesses the anti–syn coordination geometry that has been observed in other acetate-bridged polymers.[27] The syn Cd–O bond, 2.294 (4) Å, is significantly shorter than the anti Cd–O bond, 2.473 (3) Å. An ORTEP diagram of the unit cell, which contains two symmetry equivalent polymer chains passing through it which are approximately perpendicular to the *ac* plane, is shown in Figure 3.

^{113}Cd Shielding Tensor from Powder and MAS Experiments. Figure 4 (parts a and b) shows the ^{113}Cd NMR spectra of $Cd(OAc)_2(Im)_2$ (static) and spinning at 4.0 KHz, respectively. The eigenvalues of the shielding tensor can be extracted directly from the static spectrum in Figure 4a or by simulation of the MAS spectrum in Figure 4b. As shown in the inset of Figure 4b, ^{14}N ($I = 1$) couples to the ^{113}Cd ($I = 1/2$) with a coupling constant of about 150 Hz. Figure 4c is the simulated MAS spectrum of $Cd(OAc)_2(Im)_2$. The simulation ignores the consequences of dipolar coupling to ^{14}N. The ^{113}Cd shielding tensor parameters extracted from the simulation are summarized in Table II. The isotropic chemical shift of $Cd(OAc)_2(Im)_2$ is 103.4 ppm. The resonance of the model compound is within 20 ppm of the previously observed resonance of Cd-substituted carboxypeptidase-A[11] (120.0 ppm at 280 K) in the liquid state. The coordination of the $Cd(OAc)_2(Im)_2$ differs from that of Cd-substituted CPA_α[28] and native TL[29] by the presence of an additional monodentate acetate. The anisotropy of 221.38 ppm is comparable in magnitude to other mixed nitrogen and oxygen Cd compounds.[8] The asymmetry of the shielding tensor η is 0.921 and is consistent with the site symmetry of **1** for the Wyckoff[15] position e ($P2_1/c$, no. 14).

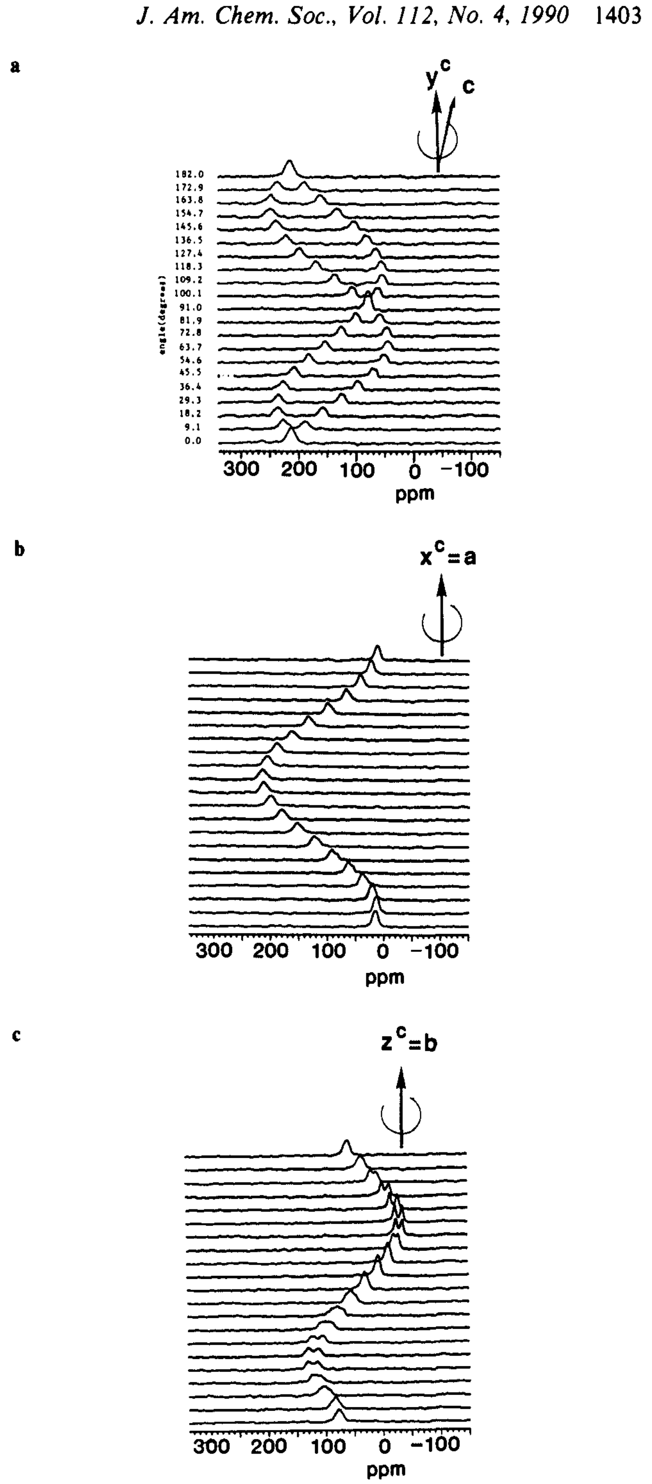

Figure 5. 66.547 ^{113}Cd single-crystal spectra of $Cd(OAc)_2(Im)_2$. The rotations plots were obtained from a single crystal of $Cd(OAc)_2(Im)_2$ (see Figure 1 for the orientation of the unit cell with respect to the cube axes) by using a Doty single-crystal orthogonal probe. a. Rotation performed about the y^c axis of the cube. The natural *c* axis is 5° off y^c of the cube. b. Rotation about the x^c axis of the cube. The natural *a* axis is collinear with x^c. c. Rotation about the z^c axis of the cube. The natural *b* axis and a 2-fold crystal axis are collinear with z^c.

Shielding Tensors from Single-Crystal NMR Experiments. The rotation plots obtained for the $Cd(OAc)_2(Im)_2$ single crystal are shown in Figure 5. The extraction of the shielding tensor from the rotation plots was accomplished by a least-squares analysis of the angular dependence of the chemical shift for each resonance and governed by eq 3[5,30]

$$\sigma^{Lab} = A + B\cos 2\alpha + C\sin 2\alpha \quad (3)$$

(25) Harrison, W.; Trotter, J. J. *J. Chem. Soc., Dalton Trans.* **1972**, 956.
(26) (a) Flook, R. J.; Freeman, F.; Huq, F.; Rosalky, J. M. *Acta Crystallogr.* **1973**, *29B*, 903. (b) Caira, M. R.; Nassimbeni, L. R.; Orpen, G. *Acta Crystallogr.* **1976**, *32B*, 140.
(27) Cotton, F. A.; Wilkinson, G. *Advance Inorganic Chemistry*; 5th ed.; Wiley: New York, 1988; pp 483–4.
(28) Rees, D. C.; Howard, J. B.; Chakrabarti, P.; Yeates, T.; Hsu, B. T.; Hardman, K. D.; Lipscomb, W. N. *Prog. Inorg. Biochem. Biophys.* **1986**, *1*, 155–166.
(29) Mathews, B. W.; Holmes, M. A. *J. Mol. Biol.* **1982**, *160*, 623.
(30) Griffin, R. G.; Ellet, J. D., Jr.; Mehring, M.; Bullitt, J. G.; Waugh, J. S. *J. Chem. Phys.* **1979**, *57*, 5, 2147.

where

$$A = \tfrac{1}{2}(\sigma_{ii}^{cube} + \sigma_{jj}^{cube})$$

$$B = \tfrac{1}{2}(\sigma_{ii}^{cube} - \sigma_{jj}^{cube})$$

$$C = \tfrac{1}{2}(-\sigma_{ji}^{cube})$$

where α is the angle of rotation of the crystal. The shielding tensor in the cube frame is transformed to the crystal frame by the following transformation matrix

$$\sigma^{c} = R(\alpha,\beta,\gamma)^{-1}\sigma^{cube}R(\alpha,\beta,\gamma) \qquad (4)$$

where $\alpha = 0°$, $\beta = 0°$, and $\gamma = 85°$ are the nontrue[31] Euler angles by which the crystal must be rotated to bring the orthogonalized unit cell axes into congruency with the orthogonal cube axes. A more comprehensive discussion of the transformation of this type and its applications to NMR have been recently elaborated by Kennedy and Ellis.[6] The principal values and the eigenvectors of the shielding tensor with respect to the crystal frame were obtained by diagonalizing σ^{c}.

Two tensors (tensor-1 and tensor-2) are evident from the rotation about the orthogonalized c axis as shown in Figure 5a. As indicated earlier the natural c axis is 5° off the y^{c} axis, Figure 1b. Tensor-1 and tensor-2 are degenerate or nearly so for a rotation about the a and b axes (Figures 5 (parts b and c)). The presence of a single resonance about the a and b of Figure 5 (parts b and c) indicate that a symmetry element is congruent with the crystal rotation axis.

Figure 6a–c shows the orientation of pairs of symmetry-related molecules for rotations about x^{c}, z^{c}, and y^{c} axes, respectively. Each molecule has been displayed with the natural axes a, b, or c normal to the plane of the paper. In Figure 6a, the rotation about the x^{c} axis indicates a rotation about the natural b axis. Since the crystallographic 2-fold axis is along the b axis and parallel with x^{c}, any crystal rotation about x^{c} will lead to degenerate resonances. In Figure 6b, the presence of a mirror which is congruent with the crystal rotation axis z^{c} will lead again to degenerate resonances. In Figure 6c, the rotation axis y^{c} is 5° off the natural c axis. Since the symmetry-related sites retain magnetically distinct orientations upon rotation about the y^{c} axis, the resonances remain distinguishable in the rotation plot of Figure 5a.

The two shielding tensors extracted from the plots of Figure 5 are summarized in Table III. An examination of the eigenvectors of tensor-1 and tensor-2 reveals that the two tensors are indeed related by a 2-fold rotation about the b axis as expected from the crystal space $P2_1/c$ for a molecule lying on a general position in the unit cell. In Figure 7 an ORTEP diagram of the two possible orientations of the shielding tensor are displayed on a $[\bar{x}y\bar{z}]$ site of the unit cell $Cd(OAc)_2(Im)_2$. Tables IV and V contains the geometric data for the shielding tensor-1, tensor-2, and the atoms of the first coordination sphere of $Cd(OAc)_2(Im)_2$.

In the extraction of tensor properties from single-crystal data, one has to be concerned with the notion of symmetry-related tensors. That is, tensors having the same eigenvalues but the eigenvectors are related by the crystallographic point group. Assignment of symmetry-related tensors to a lattice site in the crystal cannot always be made by the single-crsytal NMR experiment alone. The assignment of symmetry-related tensors to lattice sites can sometimes be made if the molecule lies on a special position within the unit cell where the site symmetry (not the molecular symmetry) imposes constraints on the orientation of the tensor.[32] With the Cd^{2+} in the general position (site symmetry = 1) of the space group $P2_1/c$ (I.T.C.,[15] no. 14) no constraints due to the site symmetry are imposed on the orientation or the symmetry of the ^{113}Cd shielding tensor of $Cd(OAc)_2(Im)_2$. The symmetry operators generate four lattice sites in the unit cell of $Cd(OAc)_2(Im)_2$ ($Z = 4$). The symmetry operators present in the $P2_1/c$ space group are the improper 2-fold rotation[18] along b, the inversion operators and a glide plane normal to b ([1] x, y, z; [2] $\bar{x}, y + \tfrac{1}{2}, \bar{z} + \tfrac{1}{2}$; [3] $\bar{x}, \bar{y}, \bar{z}$; [4] $x, \bar{y} + \tfrac{1}{2}, z + \tfrac{1}{2}$). Lattice site [1] and [3] as well as [2] and [4] are related by inversion, while [1] and [2] as well as [3] and [4] are related by an improper 2-fold[17] rotation. Since inversion-related tensors are magnetically indistinguishable, only two resonances corresponding to two symmetry-related tensors are expected from the single-crystal NMR experiment of $Cd(OAc)_2(Im)_2$.

Assignments of symmetry-related tensors to a crystal lattice site have been previously addressed[7d] by taking advantage of the coupled heteronuclear dipole–dipole interaction. This method is only useful if each site gives rise to a different angular dependence of the dipolar coupling manifested in a line width variation as a function of angle. Assignment by this method necessitates cal-

(31) Non-Euler rotation angles refer to rotations about three fixed axes rather than conventional Euler rotations about sequentially generated axes.
(32) Weil, J. A.; Buch, T.; Clapp, J. E. *Adv. Magn. Reson.* **1973**, *7*, 183.

Table III. Direction Cosine of the 2-Fold Symmetry Related Tensor Relating the Principal Elements of the ^{113}Cd Shielding Tensor to the Molecular Frame in $CdOAc_2Im_2$

		direction cosine			angles, deg		
elements	ppm[b]	c′	b′	a′	c′	b′	a′
		Tensor[a] 1					
σ_{11}	−43.7	0.7055	−0.0944	−0.7023	45	95	135
σ_{22}	95.8	0.6489	0.4842	0.5869	50	61	54
σ_{33}	248.6	−0.2847	0.8699	−0.4029	107	30	114
		Tensor[a] 2					
σ_{11}	−46.6	0.6768	0.2435	−0.6947	47	76	134
σ_{22}	104.6	−0.7332	0.3070	−0.6067	137	72	127
σ_{33}	245.0	0.0655	0.9200	0.3864	86	23	67

[a] The convention used for labeling the shielding tensor elements is after Haeberlen's *High Resolution NMR in Solids* which ascribes $\sigma_{33} = \sigma_{zz}$ = unique tensor element. [b] The ^{113}Cd chemical shifts are reported with positive values to higher shielding with respect to $Cd(ClO_4)_2 \cdot 6H_2O$.

Table IV. Structural Data for Poly(bis(acetato)bis(imidazole)cadmium(II)): Selected Interatomic Distances Angles and Geometry of Principal Elements of the ^{113}Cd Shielding Tensor-1 for the First Coordination Sphere

Interatomic Distances (Å)					
Cd2–O(1)	2.302	Cd2–O(3)	2.294	Cd2–N(1)	2.245
Cd2–O(2)	2.547	Cd2–O(4)	2.473	Cd2–N(3)	2.235

Interatomic Angles (deg)			
O(1)–Cd2–O(2)	53.2	O(2)–Cd2–N(1)	87.9
O(1)–Cd2–O(3)	90.7	O(2)–Cd2–N(3)	145.2
O(1)–Cd2–O(4)	86.1	O(3)–Cd2–O(4)	173.7
O(1)–Cd2–N(1)	140.3	O(3)–Cd2–N(1)	93.6
O(1)–Cd2–N(3)	92.2	O(3)–Cd2–N(3)	102.1
O(2)–Cd2–O(3)	84.3	O(4)–Cd2–N(1)	85.4
O(2)–Cd2–O(4)	89.5	O(4)–Cd2–N(3)	83.5
Tensor Element–Ligand Angles (deg)			
σ_{33}–Cd2–O(1)	35.7	σ_{33}–Cd2–O(4)	53.3
σ_{33}–Cd2–O(2)	72.8	σ_{33}–Cd2–N(1)	133.4
σ_{33}–Cd2–O(3)	124.8	σ_{33}–Cd2–N(3)	75.7
σ_{22}–Cd2–O(1)	95.1	σ_{22}–Cd2–O(4)	61.7
σ_{22}–Cd2–O(2)	72.8	σ_{22}–Cd2–N(1)	47.3
σ_{22}–Cd2–O(3)	113.3	σ_{22}–Cd2–N(3)	143.7
σ_{11}–Cd2–O(1)	54.6	σ_{11}–Cd2–O(4)	130.4
σ_{11}–Cd2–O(2)	44.2	σ_{11}–Cd2–N(1)	105.3
σ_{11}–Cd2–O(3)	44.0	σ_{11}–Cd2–N(3)	122.3

Table V. Geometrical Information for the Principal Elements of the ^{113}Cd Shielding Tensor-2 for the First Coordination Sphere of Polybis(acetato)bis(imidazole)cadmium(II))

tensor element–Cd–ligand angles (deg)					
σ_{11}–Cd–O(1)	39.4	σ_{22}–Cd–O(1)	125.20	σ_{33}–Cd–O(1)	74.67
σ_{11}–Cd–O(2)	30.7	σ_{22}–Cd–O(2)	72.3	σ_{33}–Cd–O(2)	65.73
σ_{11}–Cd–O(3)	63.3	σ_{22}–Cd–O(3)	76.8	σ_{33}–Cd–O(3)	149.8
σ_{11}–Cd–O(4)	111.16	σ_{22}–Cd–O(4)	100.60	σ_{33}–Cd–O(4)	23.90
σ_{11}–Cd–N(1)	110.47	σ_{22}–Cd–N(1)	22.02	σ_{33}–Cd–N(1)	82.22
σ_{11}–Cd–N(3)	123.62	σ_{22}–Cd–N(3)	142.5	σ_{33}–Cd–N(3)	104.72

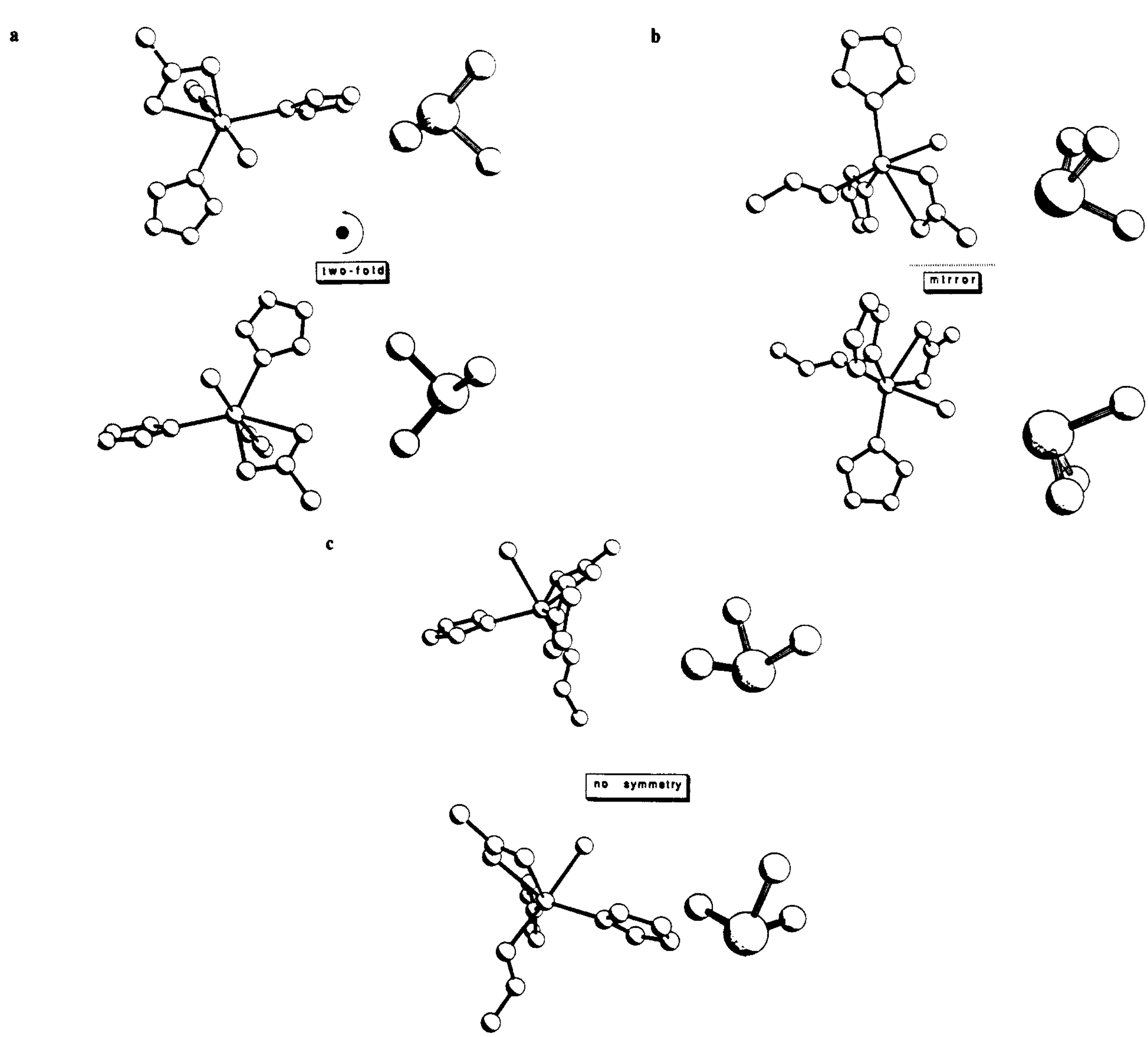

Figure 6. Represented in these sets of figures is a pair of symmetry-related molecules related in the unit cell by the crystal 2-fold rotation axis about the *b* axis. To illustrate that the crystallographic symmetry determines the symmetry properties of the shielding tensor and not the molecular symmetry a view along each unit cell axes *a*, *b*, and *c* are displayed normal to the plane of the paper in each figure. Also shown adjacent to the molecule is the preferred orientation of the shielding tensor (discussed below). a. The cube rotation axis is congruent with the natural unit cell *b*. Notice a 2-fold axis relating the molecules (this is the crystallographic 2-fold axis) and that it is congruent with the cube rotation axis. b. The cube rotation is performed about the natural *a* axis. The two molecules are related by a crystallographic mirror and are congruent with the cube rotation axis. c. The cube rotation angle is 5° off the normal of the paper (*c* axis). No crystal symmetry element relates these two sites when rotated about this axis.

culating the ^{113}Cd resonance line width contribution resulting from the dipole interaction between two nuclei using eq 5

$$\nu = \nu_0 + \frac{\gamma_{Cd}\gamma_{nucleus}}{2\pi R^3}(1 - 3\cos^2\theta)M \tag{5}$$

where R is the internuclear distances ^{113}Cd–$^{14}N(3)$ and ^{113}Cd–$^{14}N(1)$, γ is the gyromagnetic ratio of the nucleus, θ is the angle between the internuclear vectors R and the static magnetic field B_0, and M is the ^{14}N spin quantum number ($M = -2, -1, 0, 1, 2$). Initially, the assignment of the symmetry-related tensors of $Cd(OAc)_2(Im)_2$ was attempted by using the strategy discussed above by calculating the dipolar contributions to the line width that the nonbonded and bonded imidazole ^{14}N's ($I = 1$) contributes to the ^{113}Cd ($I = 1/2$) resonance. Figure 8 is a plot of the experimental ^{113}Cd resonance line width for the rotation plot of Figure 5a. In this plot the angular line width variation of the two tensors are not sufficient to allow an assignment based on this method.

An empirical approach was used to make the assignment of the tensors to the appropriate lattice site. This approach is based on empirical observations from some other model compounds where Cd is coordinated to nitrogen/oxygen ligands plus the empirical rules mentioned in the introduction.[7] In utilizing this empirical approach, the information about the best least-square planes [BLSP] of atoms in the first coordination sphere is required. The BLSP information for the two possible orientations of the shielding tensor represented in Figure 7 has been summarized in Tables VI and VII. The three planes of interest are the equatorial atoms N1/N3/O1/O2 and Cd^{2+}, the two N1/N3 and Cd^{2+}, and two bidentate O1/O2 and Cd^{2+}. For the orientation of Figure 7a, the most shielded element, σ_{11}, and the most deshielded element, σ_{33}, have nearly the same orthogonal environments with respect to the planes defined above and are shown in Table VI. A given element of the shielding tensor is a reflection of its orthogonal environment, and if σ_{11} and σ_{33} have similar orthogonal environments they should have the same magnitude (this is a case of a totally symmetric tensor). This is clearly not the case from

Table VI. Angles between the Principle Elements of the Shielding Tensor-1 and the Best Least-Squares Planes of Atoms at Site ($\hat{x}y\hat{z}$) of the Unit Cell

atoms best least-squares planes	σ_{33} (deg)	σ_{22} (deg)	σ_{11} (deg)
Cd2/N1/N3/O1/O2	35.8	29.7	−39.9
Cd2/N1/N3	−28.3	32.1	44.7
Cd2/O1/O2	−42.1	31.0	32.2

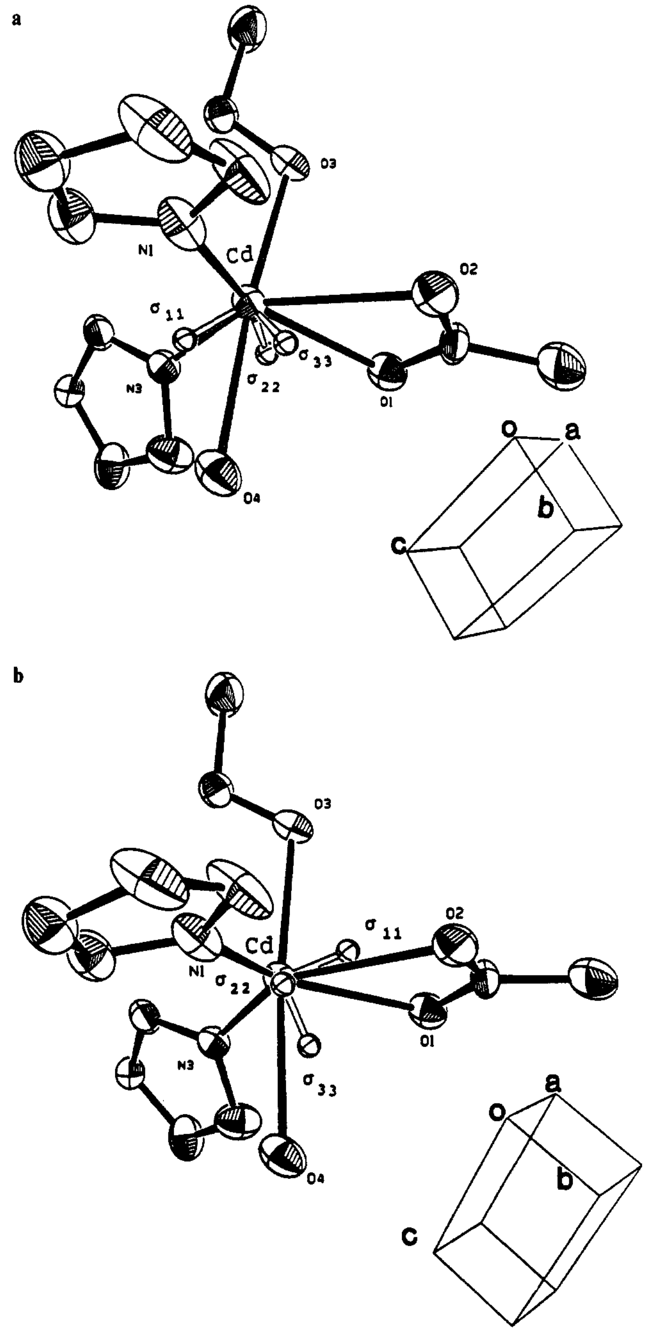

Figure 7. a. ORTEP displaying tensor-1 on $\bar{x}y\bar{z}$ site (nonpreferred). b. ORTEP displaying tensor-2 on the $\bar{x}y\bar{z}$ site (preferred). For reference the unit cell has been displayed at the bottom of the figure.

Table VII. Angles between the Principle Elements of the Shielding Tensor-2 and the Best Least-Squares Planes of Atoms at Site $\bar{x}y\bar{z}$ of the Unit Cell

atoms best least-squares planes	σ_{33} (deg)	σ_{22} (deg)	σ_{11} (deg)
Cd1/N1/N3/O1/O2	67.1	9.1	-20.8
Cd1/N1/N3	75.2	-11.5	-9.0
Cd1/O1/O2	65.6	-6.5	23.0

the single crystal and the MAS experiments discussed earlier. Therefore, the orientation shown in Figure 7a is a nonpreferred orientation.

Upon inspection of the orientation shown in Figure 7b and the BLSP data in Table VII, the most deshielded element, σ_{33}, is 75.2° from the BLSP defined by the imidazole nitrogens and Cd^{2+}, whereas the most shielded element, σ_{11}, is almost within this plane (-9.0°). σ_{11} is nearly perpendicular to the axial Cd–O bonds. This orientation does not show the discrepancy observed in Figure 7a.

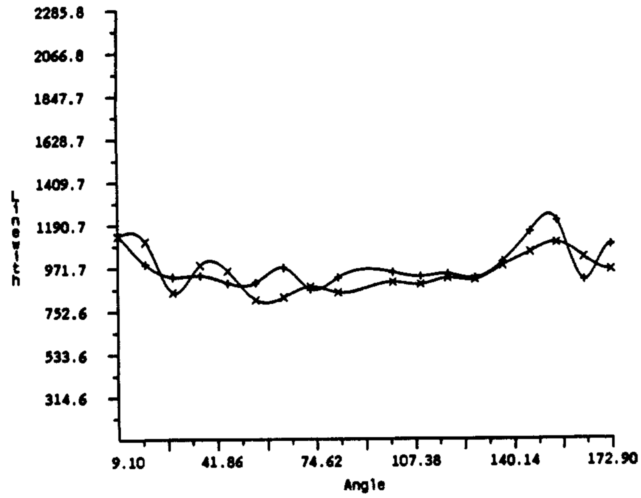

Figure 8. A plot of the experimental line width of the rotation plot of Figure 6a (crossover resonances not included), y^c. The line width is nearly invariant when the crystal is rotated about the y^c of the cube.

The orthogonal environment of σ_{11} and σ_{33} elements of the shielding tensor is distinct, and we conclude that Figure 7b represents a preferred orientation. Bolstering this suggestion is the fact that the most deshielding element, in this case σ_{33}, is most perpendicular to the most deshielding plane of atoms, i.e., bonded imidazole ^{14}N's and ^{113}Cd, indicating indeed that a shielding tensor is a reflection of its orthogonal environment.

The metal coordination of $Cd(OAc)_2(Im)_2$ differs from the reported for Cd–CPA by the presence of an additional oxygen from a bridging monodentate acetate in the model compound. In the absence of an axial monodentate acetate from $Cd(OAc)_2(Im)_2$ (now best described as a square-pyramid configuration), the structure will resemble that of CPA and TL. The orientation of σ_{33} is dominated by the plane of imidazole nitrogens. The orientation of σ_{11} is determined by the axial Cd^{2+}–O bonds. As mentioned earlier a shielding tensor is a reflection of its orthogonal environment, and, therefore, the most deshielded element σ_{33} should remain most perpendicular to deshielding planes formed by the His-69 and His-196 amino acids in the proteins. Finally, σ_{11} is within the planes formed by nitrogens and Cd(II), Table VII. The shielding tensor observed in $Cd(OAc)_2(Im)_2$ is another example in the family of recently observed Cd complexes with mixed nitrogen/oxygen bonded atoms.[8] On the basis of the arguments and observations of the ^{113}Cd shielding tensor of $Cd(OAc)_2(Im)_2$ we can now predict the orientation of the ^{113}Cd shielding tensor of Cd-substituted CPA and TL.[33]

Conclusions

The interpretation of the ^{113}Cd shielding tensor of $Cd(OAc)_2(Im)_2$ in this treatment represents another example of the utility of the NMR single-crystal experiment to study model compounds in which its metal electronic environment is representative of that of the metal site in a metalloprotein. We described the orientation of the ^{113}Cd shielding tensor of a model compound where Cd is coordinated in a mixed nitrogen/oxygen environment. In the model compound the most shielded σ_{11} element is most perpendicular to the Cd–O axial bond. The most deshielded element σ_{33} is dominated by the most deshielding plane containing the imidazole nitrogens. This model compound can be use to predict the orientation of the ^{113}Cd shielding tensor in the cadmium substituted metalloproteins, e.g., CPA and TL.

Cd-substituted CPA[28] and TL[29] have similar metal environments. With the exception of a monodentate acetate in the metal coordination of $Cd(OAc)_2(Im)_2$, the structure is comparable to that of CPA and TL. By predicting the orientation of the shielding tensor in the Cd-substituted CPA and TL valuable information can be obtained about the structural changes that take place in the metal coordination of these proteolytic enzymes upon inhibitor binding (e.g., in CPA whether or not H_2O or OH^- is displaced from the metal site upon inhibitor binding[34]). In Cd-substituted CPA, the Cd^{2+} is liganded by two histidines, a bidentate glutamate, and a water molecule. If one forms a plane that contains the Cd^{2+} and the two directly bonded nitrogen atoms from the histidines, then we have predicted[33] that σ_{33} will be nearly perpendicular to this plane, whereas σ_{11} is predicted to be nearly perpendicular to the plane of the bidentate glutamate or the water oxygen–Cd^{2+} bond. Therefore, due to the sensitivity of the shielding tensor elements to their orthogonal environments, σ_{11} and σ_{33} will be sensitive to the changes in the current density at the Cd^{2+}. Hence, if water is displaced (or not) upon inhibitor binding, this fact should be reflected in the NMR line shape for the Cd^{2+} nucleus. Further discussion about the orientation of the ^{113}Cd shielding tensor for this model compound in relation to Cd-substituted carboxypeptidase-A is addressed elsewhere.[33]

(33) Rivera, E.; Kennedy, M. A.; Ellis, P. D. *Adv. Magn. Reson.* Academic Press: 1989; Vol. 13, pp 257–273.

Acknowledgment. This work was partially supported by grants from the National Institutes of Health, GM 26295 and MARC predoctoral fellowship GM-09585 (E.R.). Many of the calculations discussed here were performed on a Microvax II computer obtained via an award from NSF, CHE86-13421. We also thank Dr. Shen-il Cho for his assistance in the electronic aspects of the single-crystal experiments. We also thank Dr. E. L. Amma of the Chemistry Department of the University of South Carolina for the use of the X-ray camera equipment necessary for the crystal alignment.

Supplementary Material Available: Tables containing details of the structure determination and refinement, anisotropic thermal parameters, bond distances and angles, and hydrogen atom positions for $Cd(OAc)_2(Im)_2$ (4 pages). Ordering information is given on any current masthead page.

(34) Mock, W. L.; Tsay, J.-T. *J. Am. Chem. Soc.* **1989**, *111*, 4467.

Why Is SiH_5^- a Stable Intermediate while CH_5^- Is a Transition State? A Quantitative Curve Crossing Valence Bond Study

Gjergji Sini,[1a] Gilles Ohanessian,[1a] Philippe C. Hiberty,*[,1a] and Sason S. Shaik*[,1b]

Contribution from the Laboratoire de Chimie Théorique,† Bât. 490, Université de Paris-Sud, 91405 Orsay Cedex, France, and the Department of Chemistry, Ben-Gurion University of the Negev, Beer-Sheva, 84105, Israel. *Received September 12, 1988*

Abstract: Valence bond computations of curve-crossing diagrams reveal a fundamental difference between the title species. The stability of SiH_5^- does not derive from hypervalency associated with d-AOs on Si but rather from the ability of Si to utilize its Si–H σ^* orbitals for bonding, much more so than C does with its σ^*(C–H) orbitals. Consequently, SiH_5^- possesses *two* resonating H- -Si- -H axial bonds; one via the axial p-AO of Si and the other via the equatorial $\sigma^*(SiH_3)$ orbital of the central SiH_3 fragment. As a result of the bonding capability of $\sigma^*(SiH_3)$, SiH_5^- can delocalize efficiently the fifth valence-electron pair into the equatorial Si–H bonds. The energy of SiH_5^- is thus lowered by the delocalization relative to $SiH_4 + H^-$. No significant stretching of the axial bonds is required to achieve this delocalized state, and therefore the bond lengths of SiH_5^- do not exceed those of SiH_4 by much. On the other hand, the $\sigma^*(CH_3)$ orbital possesses no bonding capability. The analogous delocalization of the fifth valence-electron pair is prohibited by the high promotion energy p $\rightarrow \sigma^*$ and by the nearly zero overlap of $\sigma^*(CH_3)$ with the axial hydrogens. As an alternative, CH_5^- localizes its fifth valence electron into the axial H- -C- -H linkage. This option leads to a long H- -C- -H linkage and a high energy of CH_5^- relative to $CH_4 + H^-$.

A fundamental chemical phenomenon is the different nature of the S_N2-type reactions at carbon and silicon.[2] This difference is exemplified in the simplest of these reactions, the H- exchange in eqs 1 and 2.[3]

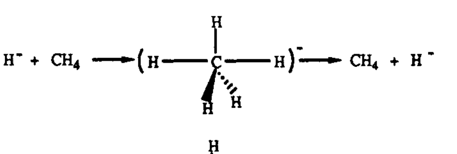
(1)

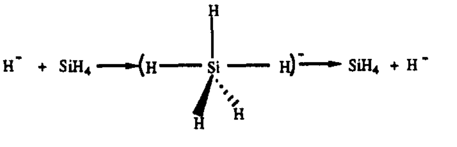
(2)

These two reactions are isoelectronic in terms of valence electrons and isostructural in terms of the geometric types of the main species along the reaction coordinate. Despite these similarities, the two reactions are quantitatively different. Thus, in reaction 1, the trigonal-bipyramidal CH_5^- is a high-energy transition state,[3,4] lying some 52–64 kcal/mol above the reactants and products, depending on the level of calculation. On the other hand, in reaction 2 the trigonal bipyramidal structure, recently synthesized and characterized in a gas-phase reaction,[5] is an intermediate,[3,4b,c,5–8] 13–20 kcal/mol lower than reactants and products, depending on the method of estimation.[4b,6–8]

What is the origin of this qualitative difference between the S_N2 chemistries of carbon and silicon?[2–9] One possible explanation is the participation of d-orbitals which endow Si with aptitude for pentacoordination.[2c,4c,5] However, at least for SiH_5^-,

†The Laboratoire de Chimie Théorique is associated with the CNRS (URA 506).

(1) (a) Université de Paris-Sud. (b) Ben-Gurion University.
(2) (a) Corriu, R. J. P.; Dabosi, G.; Martineau, M. *J. Organomet. Chem.* **1980**, *186*, 25. (b) Stevenson, W. H.; Martin, J. C. *J. Am. Chem. Soc.* **1985**, *107*, 6352. (c) Corriu, R. J. P.; Guerin, C. *Adv. Organomet. Chem.* **1982**, *20*, 26. (d) Corriu, R. J. P.; Guerin, C. *J. Organomet. Chem.* **1980**, *198*, 231.
(3) Payzant, J. D.; Tanaka, K.; Betovski, L. D.; Bohme, D. K. *J. Am. Chem. Soc.* **1976**, *98*, 894.
(4) See for example: (a) Dedieu, A.; Veillard, A. *J. Am. Chem. Soc.* **1972**, *94*, 6730. (b) Baybutt, P. *Mol. Phys.* **1975**, *29*, 389. (c) Keil, F.; Ahlrichs, R. *J. Am. Chem. Soc.* **1972**, *94*, 6730. (d) Wolfe, S.; Mitchell, D. J.; Schlegel, H. B. *J. Am. Chem. Soc.* **1981**, *103*, 7694.
(5) Hajdasz, D. J.; Squires, R. R. *J. Am. Chem. Soc.* **1986**, *108*, 3139.
(6) Wilhite, D. L.; Spialter, L. *J. Am. Chem. Soc.* **1973**, *95*, 2100.
(7) Reed, A. E.; Schleyer, P. v. R. *Chem. Phys. Lett.* **1987**, *133*, 553.
(8) Keil, F.; Ahlrichs, R. *Chem. Phys.* **1975**, *8*, 384.
(9) For discussions see: Anh, N. T.; Minot, C. *J. Am. Chem. Soc.* **1980**, *102*, 103.

0002-7863/90/1512-1407$02.50/0 © 1990 American Chemical Society